Phase diagram of CeCu$_2$(Si$_{1-x}$Ge$_x$)$_2$

G. Knebel, C. Eggert, D. Engelmann, R. Viana, A. Krimmel,* M. Dressel,† and A. Loidl

Institut für Festkörperphysik, Technische Hochschule Darmstadt, Hochschulstraße 6, D-64289 Darmstadt, Germany

The magnetic phase diagram of the system CeCu$_2$(Si$_{1-x}$Ge$_x$)$_2$ with $0 \leq x \leq 1$ is studied by electrical transport, magnetic susceptibility, and neutron scattering measurements. The transition from heavy-fermion superconductivity in CeCu$_2$Si$_2$ to the local moment type of antiferromagnetism in CeCu$_2$Ge$_2$ is explored. The system reveals a rich phase diagram with up to three distinct transitions below 5 K. The nature of the phases is not fully resolved yet.

I. INTRODUCTION

Since the first discovery of superconductivity,[1] the heavy-fermion compound CeCu$_2$Si$_2$ has been studied intensively. But still this system reveals new and exciting phenomena as the B-T phase diagram shows which was recently discovered by elastic and thermodynamic investigations[2] as well as by muon spin relaxation (μSR) experiments.[3,4] In contrast to U-based heavy-fermion superconductors, the superconducting phase of CeCu$_2$Si$_2$ does not coexist with the surrounding magnetic phase. The so-called A phase at moderate magnetic field, which exhibits magnetic signatures of an as yet unclear nature, is expulsed by the onset of superconductivity ($T_c = 0.63$ K). In addition to the A phase, a second phase (labeled B) occurs in high magnetic fields above 7 T.[5] Both phases, A and the high-field phase B, develop out of a state which is characterized by a T^2 law of the resistivity indicating heavy-Fermi-liquid behavior.[6]

In CeCu$_2$Ge$_2$, which is isostructural to CeCu$_2$Si$_2$, the energy scales of the RKKY and Kondo-type interactions are of the same order. CeCu$_2$Ge$_2$ is antiferromagnetic (AFM) ($T_N = 4.1$ K),[7] and superconductivity (starting at $T_c = 0.7$ K) can only be induced by applying an external pressure of more than 70 kbar.[8] At ambient pressure and low temperatures, the $4f$ moments are partially Kondo compensated but still well localized. Below the Néel temperature T_N they reveal an incommensurably modulated magnetic order.[7] Investigations of ^{63}Cu NMR yield information on the local magnetic behavior of CeCu$_2$Ge$_2$.[9] For $T \gtrsim T_N$, the nuclear relaxation rate $1/T_1$ is dominated by the intersite magnetic interaction of RKKY type with a vanishing on-site contribution of Korringa type. In addition, these NMR experiments report the opening of a spin gap in the AFM phase.[9] The antiferromagnetic energy gap was also found by measurements of the thermoelectric power[8] and neutron scattering.[7] Recent NMR nuclear quadrupole resonance (NQR) studies on CeCu$_2$Ge$_2$ performed under high pressure provide evidence that above the transition from the AFM to the superconducting phase, which takes place at 76 kbar, the physical properties of CeCu$_2$Ge$_2$ are clearly related to those of CeCu$_2$Si$_2$ at ambient pressure.[10] As the hybridization between $4f$ and conduction electrons increases, the antiferromagnetism is depressed, and heavy-electron superconductivity emerges. The p-T phase diagram shown in Ref. 10 and

the B-T phase diagram[2–4] call for completion. Specifically, the nature of the A and B phases is yet unknown. In addition, in careful studies with almost stoichiometric compositions of CeCu$_2$Si$_2$, an X phase has been detected which is lacking any phase transition.[6] The present studies were guided by the expectation that alloying experiments may contribute to our understanding of these complex phases.

Alloying has proven to be a useful way for studying the competition between the on-site (Kondo) and intersite (RKKY) interactions typically found in heavy-fermion systems. One of the important examples is the compound Ce(Cu$_{1-x}$Ni$_x$)$_2$Ge$_2$ which shows a transition from a local-moment type of AFM ordering for $x \leq 0.5$ to a heavy-fermion band magnetism between $x \approx 0.5$ and $x \approx 0.7$ (Ref. 11) and finally to a heavy Fermi liquid close to the CeNi$_2$Ge$_2$ subsystem.[12] In the local-moment regime, two subsequent phase transitions were reported. In order to discriminate between effects of chemical substitution, e.g., electronic band-structure effects, and effects on the strength of the $4f$ ligand hybridization, measurements of specific heat and resistivity of Ce(Cu$_{1-x}$Ni$_x$)$_2$Ge$_2$ have been performed under pressure.[13] The Kondo temperature T_K was found to be governed by volume, while the sequence of magnetic ordering temperatures could not be reproduced in CeCu$_2$Ge$_2$ by a corresponding change in volume. It has been concluded that the higher transition indicates the ordering of local moments while the lower transition reflects a reorientation of the magnetic moments within the antiferromagnetically ordered phase. A recent study[14] of the system Ce(NiSi)$_{2-x}$(CuGe)$_x$ indicated a smooth transition from a highly mixed-valence system to a magnetically ordered Kondo-lattice system as x goes from 0 to 2.

To illuminate the transition from a local-moment type of antiferromagnetism to a heavy-fermion superconductor, we investigated the quasibinary system CeCu$_2$(Si$_{1-x}$Ge$_x$)$_2$ in the entire range from $x = 0$ to $x = 1$. Early studies[15] show that the superconducting transition temperature in CeCu$_2$(Si$_{1-x}$Ge$_x$)$_2$ decreases from $T_c \approx 0.6$ K to $T_c < 0.1$ K as x increases to only 5%. Since substituting Si with the larger Ge atoms introduces a kind of negative pressure, this agrees with the large enhancement of T_c from 0.7 K to 2.2 K upon increasing pressure to $p = 30$ kbar in CeCu$_2$Si$_2$,[16,17] although the shift is not continuous. The effect of replacing Si by Ge atoms in the system CeCu$_2$(Si$_{1-x}$Ge$_x$)$_2$ is twofold. First, the size of the atoms is varied; hence the internal (or

TABLE I. Result of the Rietveld refinement in CeCu$_2$(Si$_{1-x}$Ge$_x$)$_2$. Nominal Ge concentration x and refined values x_{ref}, lattice parameters a, c, and z, and R values.

x	T (K)	x_{ref}	a (Å)	c (Å)	z	R_{Bragg} (%)	R_F (%)
0.4	1.6	0.428(9)	4.0911(24)	9.9078(116)	0.3745(26)	9.14	5.71
	7.3	0.438(9)	4.0916(25)	9.9091(119)	0.3751(27)	9.76	5.35
0.6	1.6	0.605(2)	4.1055(6)	10.0065(18)	0.3792(4)	4.50	2.59
	27.0	0.599(2)	4.1059(6)	10.0100(19)	0.3781(5)	6.28	3.67
0.8	1.6	0.853(2)	4.1179(6)	10.0682(19)	0.3757(5)	3.92	3.19
	27.0	0.859(2)	4.1179(6)	10.0687(19)	0.3755(5)	3.26	2.37

chemical) pressure is reduced. Second, the replacement of Si by Ge changes the electronic density of states at the Fermi level. By comparison with pressure studies the influence of both effects may be separated.

We performed studies of the magnetic susceptibility, dc electrical transport measurements, and neutron scattering investigations on polycrystalline $CeCu_2(Si_{1-x}Ge_x)_2$ in the temperature range from 70 mK to 300 K. From these experiments a complex x-T phase diagram is constructed and we speculate on the nature of the different phases observed. A similar phase diagram has recently been obtained on the basis of heat capacity experiments.[18]

II. SAMPLE CHARACTERIZATION

The samples of CeCu$_2$(Si$_{1-x}$Ge$_x$)$_2$ were prepared by repeated arc melting of appropriate quantities of the constituent elements in an argon atmosphere. Since it is established[15,19] that a 10% Cu excess leads to the highest superconducting transition temperature in the system CeCu$_{2+y}$Si$_2$, we conclude that these samples are closest to the ideal CeCu$_2$Si$_2$ composition. Therefore all the samples of the series were made with a slight nominal excess of Cu ($y=0.2$). Microprobe and x-ray powder diffraction techniques confirmed the specimens to be single phase and to crystallize in the proper body-centered-tetragonal ThCr$_2$Si$_2$ structure.

As predicted by Vegard's law, both lattice parameters increase roughly linear with x: We find a to increase from 4.10 Å to 4.17 Å, and c from 9.91 Å to 10.2 Å. The change $\Delta c/c$ is about twice the change $\Delta a/a$ in agreement with two (Si,Ge) atoms per unit cell in the c direction compared to one in the a direction. As x approaches 1, we observe a slower increase of a while the $c(x)$ curve remains strictly linear. These findings are in accordance with the lattice parameters in the CeMn$_2$(Si$_{1-x}$Ge$_x$)$_2$ series.[20] In Ce(Ni$_{1-x}$Cu$_x$)$_2$Si$_2$, however, Vegard's law is well observed[21,22] for the a direction and slight deviations are found in c. In agreement with the results of both series, the double substitution[14] in Ce(NiSi)$_{2-x}$(CuGe)$_x$ exhibits deviations from the linear dependence in both directions; i.e., it is seen that the two effects simply add up.

Increasing the Ge concentration x leads to a statistical substitution of Si, accompanied by an increase in unit-cell volume from $V=166.4$ Å^3 in $x=0$ to $V=176.2$ Å^3 in the compound with $x=1$. In this sense Ge alloying acts like negative chemical pressure, in accordance with studies of CeCu$_2$Ge$_2$ under hydrostatic pressure,[10] where basically the

properties of CeCu$_2$Si$_2$ are recovered. At low temperatures ($T=1.6$ K), we also determined the lattice parameters of CeCu$_2$(Si$_{1-x}$Ge$_x$)$_2$ by neutron powder diffraction measurements. The results are listed in Table I.

III. EXPERIMENTAL RESULTS AND ANALYSIS

A. Susceptibility

The magnetic susceptibility was studied in the temperature range from 2.4 to 300 K by a vibrating-sample magnetometer similar to the one described by Foner.[23] In addition, between 1.8 and 40 K the susceptibility of polycrystalline samples of CeCu$_2$(Si$_{1-x}$Ge$_x$)$_2$ was measured in a field of 0.1 mT by the standard ac susceptibility technique (1 kHz).

The inverse susceptibility χ^{-1} of CeCu$_2$(Si$_{1-x}$Ge$_x$)$_2$ is plotted in Fig. 1 as a function of temperature for $x=0.2$ and 0.9. According to the Curie-Weiss law

$$\chi(T) = \frac{N\mu_{eff}^2}{3k_B(T+\Theta)}, \tag{1}$$

$\chi^{-1}(T)$ follows a straight line from room temperature down to 40 K or lower for all Ge concentrations $0 \leq x \leq 1$. An increased slope of $\chi^{-1}(T)$ is found in the range between the Néel temperature T_N and 25 K. In the inset of Fig. 1, the Curie-Weiss temperatures Θ obtained from the fits of the high-temperature susceptibilities are displayed as a function of x. The Curie-Weiss temperature decreases linearly from
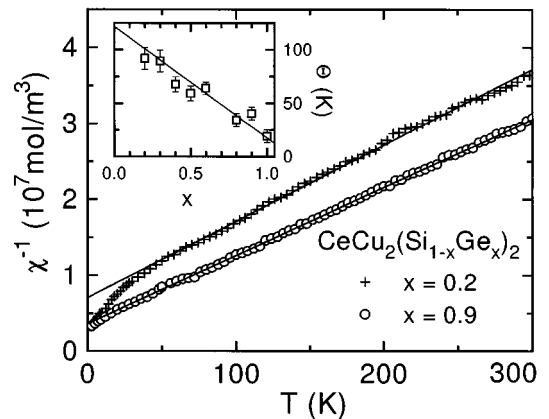
FIG. 1. The inverse magnetic susceptibility $\chi^{-1}(T)$ of CeCu$_2$(Si$_{1-x}$Ge$_x$)$_2$ as a function of temperature for two concentrations $x=0.2$ and 0.9. The inset shows the Curie temperature Θ vs concentration obtained from the high-temperature data.
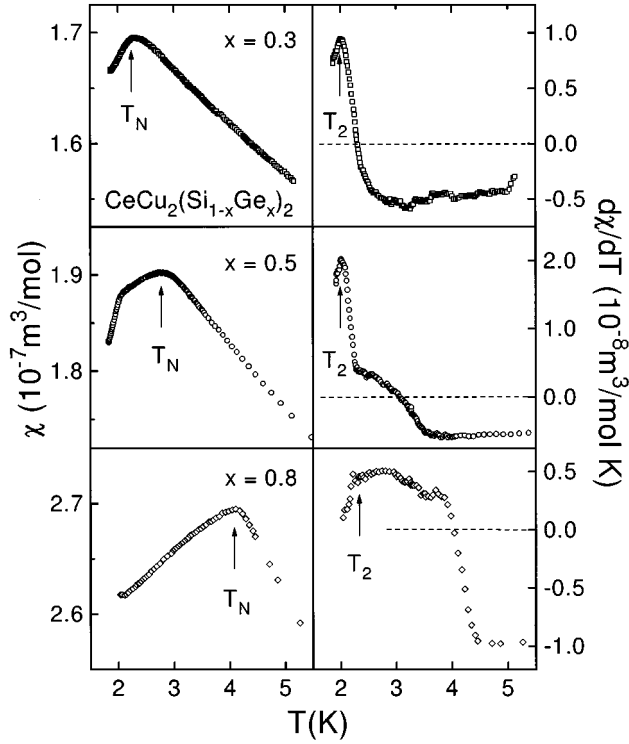
FIG. 2. Magnetic susceptibility χ vs temperature T of $CeCu_2(Si_{1-x}Ge_x)_2$. The right panels show the corresponding derivatives $d\chi/dT$. The maximum of $\chi(T)$ defines T_N; another transition T_2 is seen by the peak of $d\chi/dT$.

$\Theta \approx 140$ K ($CeCu_2Si_2$) to $\Theta \approx 20$ K ($CeCu_2Ge_2$). It will be documented in the following that T_N increases from 1 K close to $CeCu_2Si_2$ to 4 K in pure $CeCu_2Ge_2$. It is obvious that the Curie-Weiss temperature Θ is dominated by the single-ion Kondo effect rather than by the magnetic exchange interactions. This will be discussed in Sec. IV in detail.

For all values of $x > 0$, a maximum in $\chi(T)$ was found at low temperatures. The absolute value of χ increases with x by less than a factor of 2. In Fig. 2 the low-temperature part of the susceptibility for $x = 0.3$, 0.5, and 0.8 is shown in order to enlarge the maximum of $\chi(T)$ at T_N. In addition, the derivative $d\chi/dT$ is evaluated and displayed in the corresponding plots of Fig. 2; this allows us to detect anomalies in the ac susceptibility. The Néel temperature is defined by the cusp maximum of $\chi(T)$, corresponding to the zero crossing of $d\chi/dT$. A second anomaly at T_2 is indicated by the change of slope, best seen as a maximum in the derivative.

In Fig. 3 the change in susceptibility $d\chi/dT$ is compared with the heat capacity C_p/T at similar concentrations.[18] We can clearly identify three distinct types of temperature dependences of $d\chi/dT$ and find the same pattern in C_p/T. Figure 3 clearly indicates the same sequence and pattern of phase transitions from heat capacity and susceptibility measurements. Since the results of the two methods were obtained from samples of different laboratories, they indicate a general and intrinsic behavior. For low Ge concentration, only one maximum at low temperatures (T_N) is seen. In the intermediate regime ($0.4 \leq x \leq 0.6$) a broad shoulder builds up on the higher-temperature side, leading to a double feature consisting of a narrow T_2 peak which moves to slightly
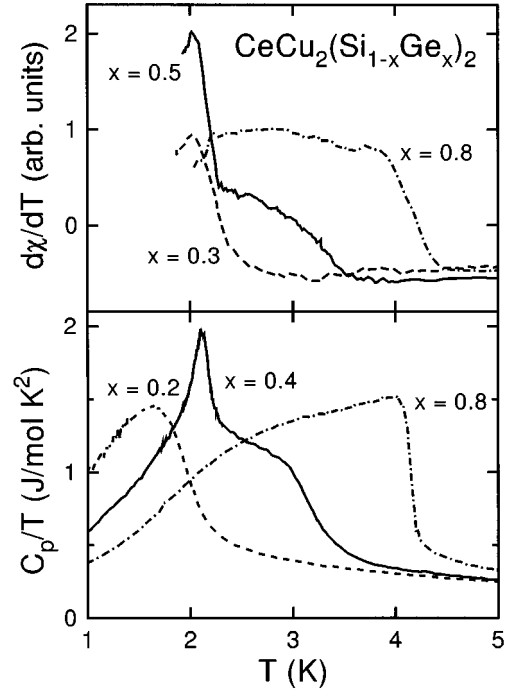
FIG. 3. The derivative of the susceptibility $d\chi/dT$ (shifted for clarity) exhibits a similar temperature dependence as the heat capacity C_p/T [data taken from Trovarelli *et al.* (Ref. 18)]: For small x (up to $x \approx 0.3$), there is a single maximum at low temperatures. In the intermediate range ($0.4 \leq x \leq 0.7$), the peak shifts to higher temperatures and gets narrower; in addition a shoulder is seen at the high-temperature side. For large x, a broad maximum is found with an almost flat top and a sharp drop at T_N.

lower temperatures as x increases, and broad flat-top band which gets more pronounced for larger x. Above $x = 0.8$ no indications of T_2 can be found in the susceptibility data down to 1.8 K.

B. Resistivity

In the temperature range from 70 mK to 300 K, we performed measurements of the electrical resistivity on $10 \times 1 \times 1$ mm³ bulk samples cut from ingots of $CeCu_2(Si_{1-x}Ge_x)_2$ ($0 \leq x \leq 1$) using a standard four-probe lock-in technique. The normalized resistivity of $CeCu_2(Si_{1-x}Ge_x)_2$ is plotted in Fig. 4 as a function of temperature for different Ge concentrations. The absolute value $\rho(300$ K$)$ falls between 100 and 200 $\mu\Omega$ cm without a significant dependence on x.

For all concentrations, a distinct double-peak feature can be seen: one at 100 K and a second one around 10 K. The broad but well-defined maximum around $T_{CF} \approx 100$ K is due to the crystal field (CF) excitations and does not change its temperature appreciably with variation of x. Lowering the temperature leads to a more or less pronounced minimum of the resistivity at $T_{min} \approx 30$ K. The low-temperature maximum defines the Kondo-lattice temperature T^* which depends on the concentration and can barely be seen for small x, because it almost merges with the CF-derived peak. As usually observed, for heavy-fermion systems with Kondo-lattice temperatures $T^* \gtrsim 30$ K, the Kondo and CF peaks cannot be separated any more. From these results, we conclude
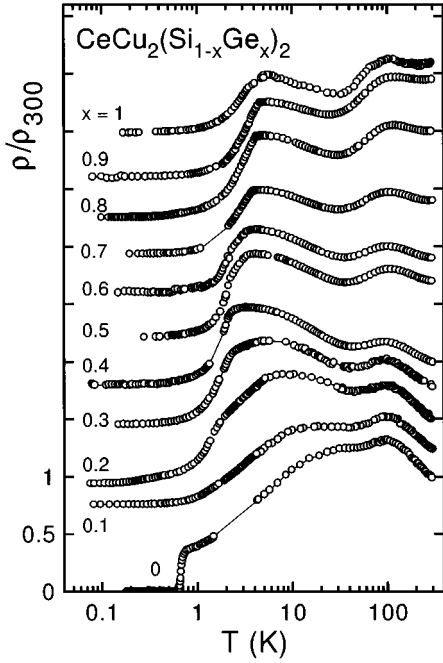
FIG. 4. The temperature dependence of the normalized resistivity $\rho(T)/\rho(300\ \mathrm{K})$ of CeCu$_2$(Si$_{1-x}$Ge$_x$)$_2$ for $0 \leq x \leq 1$. The room temperature resistivity $\rho(300\ \mathrm{K})$ is typically $10^{-4}\ \Omega$ cm, independent of x. The curves for different x are displaced for clarity.

that T^* decreases rapidly from $x=0$ up to $x=0.4$, and then to rise slowly for higher Ge concentrations. The ratio $\rho(T^*)/\rho(T_{\mathrm{CF}})$ decreases as the Ge concentration increases and we find $\rho(T^*)/\rho(T_{\mathrm{CF}}) < 1$ for concentrations $x > 0.7$. The low-temperature $\rho(T)$ of CeCu$_2$(Si$_{1-x}$Ge$_x$)$_2$ is displayed in Fig. 5 for some values of x. A close look reveals that the electrical resistivity is not smooth below $T = 5$ K and the structure in $\rho(T)$ is assumed to be related to phase transitions. In order to illustrate the anomalies in $\rho(T)$, the derivative is plotted as a function of temperature as well: A jump in $d\rho/dT$ corresponds to a change in slope, and a maximum indicates a rapid drop of $\rho(T)$. In general, we used the extrema in $d\rho/dT$ to determine the transition temperatures. On the Si-rich side $x \leq 0.3$, $d\rho/dT$ contains two peaks. While the higher-temperature feature (around 2 K) slowly moves to larger T with increasing x and can be correlated with T_2, the low-temperature anomaly remains at $T_3 \approx 0.5$ K for all x. In the intermediate range ($0.4 \leq x \leq 0.8$), we find a broad underlying structure building up in $d\rho/dT$ which at $x = 0.8$, for instance, dominates the range from 2 to 4.5 K and makes the T_2 feature vanish.

The so-obtained transitions temperatures together with the anomalies found by the susceptibility experiments are used to construct the x-T phase diagram shown in Fig. 6.

C. Neutron diffraction

Elastic neutron scattering experiments were performed on polycrystalline CeCu$_2$(Si$_{1-x}$Ge$_x$)$_2$ to investigate the magnetic structure and the size of the ordered moment. Powder patterns for $x=0.4$, 0.6, and 0.8 were recorded using the multidetector diffractometers E3 and E6 located at the BENSC in the Hahn-Meitner Institut Berlin. Carefully pow-
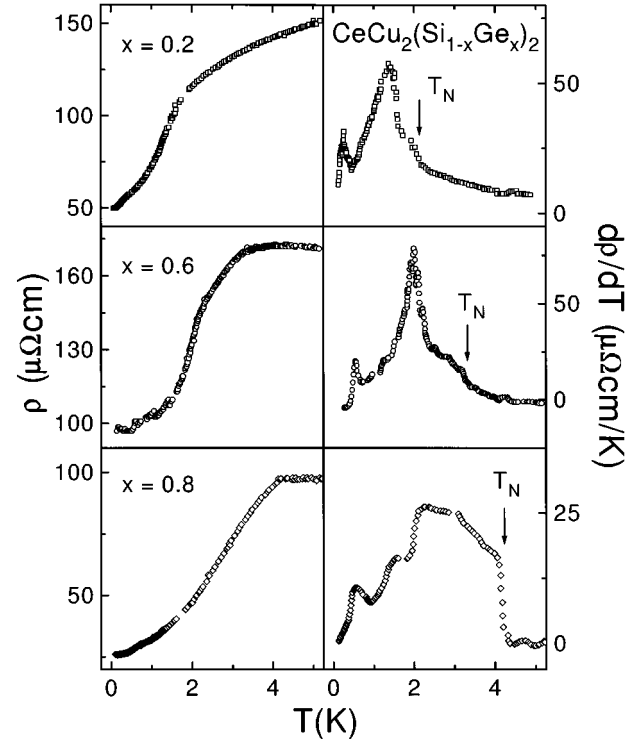
FIG. 5. The resistivity of CeCu$_2$(Si$_{1-x}$Ge$_x$)$_2$ as a function of temperature is shown in the low-temperature region for different concentrations of Ge as indicated. The right panels exhibit the corresponding slope $d\rho/dT$. The arrows indicate the Néel temperature, and the peaks of $d\rho/dT$ identify the anomalies at T_2 and T_3.

dered samples were filled in vanadium containers and mounted in orange-type cryostats. The multidetectors covered an angular range from $5°$ to $85°$ for both diffractometers. Incident neutron wavelengths of $\lambda = 2.4409$ Å (E3) and
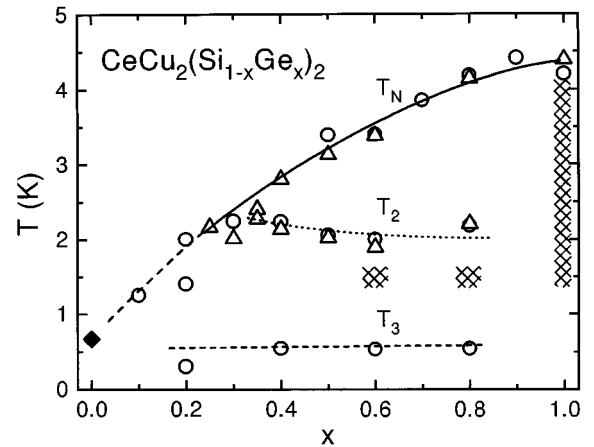
FIG. 6. Phase diagram of CeCu$_2$(Si$_{1-x}$Ge$_x$)$_2$. The open circles indicate the anomalies observed in the resistivity data; the triangles are obtained by susceptibility measurements; the solid diamond represents the superconducting transition in CeCu$_2$Si$_2$. The solid line indicates the Néel temperature T_N. In addition two critical temperatures T_2 and T_3 can be identified. The hatched area represents the regions of similar magnetic structure observed by neutron diffraction.

TABLE II. Propagation vectors $\vec{q}_0$ and ordered moments μ_s for $CeCu_2(Si_{1-x}Ge_x)_2$ at $T \approx 1.6$ K.

x	$\vec{q}_0$	μ_s/μ_B
0.4	—	<0.25
0.6	(0.271, 0.271, 0.520)	0.36 ± 0.15
0.8	(0.269, 0.269, 0.550)	0.46 ± 0.15
1.0	(0.28, 0.28, 0.53)	1.05 ± 0.1

$\lambda = 2.41663$ Å (E6) were selected by pyrolytic graphite monochromators. The measurements were performed at temperatures $T \geqslant T_N$ and in the magnetically ordered state at 1.6 K.

All samples exhibit the $ThCr_2Si_2$ structure with no indications of spurious phases. The nuclear structures were analyzed using standard Rietveld techniques. The lattice constants a, c, and z, where z is the reduced coordinate of the (Ge, Si) atoms in the tetragonal cell, were refined. In addition, the occupation number, i.e., the Ge concentration x, is treated as a free parameter. The results of the Rietveld refinement, together with the R values R_{Bragg} and R_F, are listed in Table I.

To determine the magnetic structures the difference spectra were analyzed. Here the intensities as measured in the paramagnetic phase were subtracted from the spectra in the magnetically ordered phases at 1.5 K. The spectra for $x = 0.8$ and $x = 0.6$ look very similar to what was observed in $CeCu_2Ge_2$.[7] No magnetic intensities could be detected for $x = 0.4$.

All magnetic intensities are very weak and the peak positions are incompatible with a simple commensurate structure. The Bragg angles of the magnetic reflections can be indexed in terms of $|\vec{Q}| = \vec{\tau}_{hkl} \pm \vec{q}_0$ where $\vec{\tau}_{hkl}$ is a vector of the reciprocal nuclear lattice. The propagation vectors $\vec{q}_0$ are determined graphically and by trial and error. Then a group theoretical analysis following the classical paper by Bertaut[24] was performed in order to extract all possible magnetic structures in accordance with the propagation vector. Finally, having established all possible structures allowed by the symmetry, the intensities were fitted using the MINREF program.[25] This procedure was also used for reanalyzing pure $CeCu_2Ge_2$.[7] The fits indicate collinear spin arrangements with a modulation of the length of the magnetic moments. The spins are confined to the [110] plane. However, as the $(000)^{\pm}$ reflection can be detected for $x = 0.6$, 0.8, and 1.0, the spins cannot point along $\vec{q}_0$. The best fits reveal that the direction of the spins is inclined by about 10° ($x = 1$) to 20° ($x = 0.6$) with respect to the propagation vector. The propagation vectors and the ordered moments are summarized in Table II. The fact that no magnetic Bragg reflections could be detected for $x = 0.4$ can be used as a rough estimate for the upper limit of the ordered moment ($\mu_s < 0.25\mu_B$). For $x = 0.6$, 0.8, and 1.0, the propagation vectors are very similar. The main effect of Si substitution is an increased compensation of the localized moments. With respect to the phase diagram presented in Fig. 6 two facts have to be noted. For $x = 1$, the magnetic Bragg reflections are measured from 1.5 K to 4.1 K, indicating no further magnetic phase transitions.[7] The present measurements for $x = 0.8$ and 0.6

were taken at 1.6 K, well below the phase line T_2. Hence, the crosshatched area in Fig. 6 defines regions of the phase diagram with essentially the same magnetic structure.

The fact that the magnetic structure in $CeCu_2(Si_{1-x}Ge_x)_2$ is amplitude modulated rather than an equal moment spiral is also enforced by the heat capacity results.[18] In amplitude-modulated structures, the jump of the specific heat at the phase transition temperature is reduced by 33% (Refs. 26,27) because the spins close to the nodes of the modulation are almost paramagnetic and therefore do not contribute to the specific heat. This reduction of C_p at T_N increases the heat capacity at low temperatures, leading to a broad *humplike* feature to compensate for the loss of entropy at T_N.

IV. DISCUSSION

The broad peak of the electrical resistivity at T_{CF} is caused by the interplay of Kondo scattering and the crystal fields of the $4f$ electrons. According to the symmetry of the Ce^{3+} ions in the $ThCr_2Si_2$ structure, one expects the $J = 5/2$ ground multiplet to be split into three doublets. In $CeCu_2Ge_2$ a doublet ground state is followed by a pseudo-quartet with an energy splitting $\Delta/k_B \approx 190$ K.[7] A similar CF splitting was observed by Goremychkin and Osborn[28] in $CeCu_2Si_2$ ($\Delta/k_B = 240$ K). The fact that within the experimental uncertainty T_{CF} remains unaffected by alloying gives evidence that the crystal-field splitting stays almost constant for all x. Levy and Zhang[29] have shown that in heavy-fermion systems the hybridization alone can account for the magnitude of the CF splitting. In $CeCu_2(Si_{1-x}Ge_x)_2$ the Kondo-lattice temperature increases from $T^* = 6$ K ($x = 1$) to $T^* = 15$ K ($x = 0$) while the CF splitting is almost concentration independent. It would be interesting to compare the model of Levy and Zhang[29] to these results.

Due to the onset of Kondo scattering below T_{min}, $\rho(T)$ increases as the temperature is further reduced. In this range the resistivity follows a $\rho(T) \propto -\ln T$ behavior which is typical for a single-ion Kondo type of scattering.[30] The negative thermopower below 50 K also indicates a spin interaction and allows one to ascribe the minimum to Kondo scattering on the crystal-field ground state.[8] The low-temperature peak in $\rho(T)$ can roughly be taken as a measure of the characteristic Kondo-lattice temperature T^*. As displayed in Fig. 4, the maximum corresponding to T^* remains almost constant for $0.5 \leqslant x \leqslant 1$ [$T^* \approx 5$ K; for concentrations close to $x = 1$, the maximum in $\rho(T)$ closely corresponds to the onset of magnetic order]. For $x < 0.5$, it shifts to higher temperatures, reaching 25 K for $x = 0$. It is interesting to note that a similar $T^*(x)$ behavior can be deduced from the magnetic susceptibility. The Curie-Weiss temperature Θ extracted by using Eq. (1) and plotted as a function of x in the inset of Fig. 1 decreases from 100 K ($x = 0.2$) to 20 K ($x = 1$) linearly with concentration. Grüner and Zawadowski[31] have shown that the Kondo temperature can be found from $\chi(T)$ data as $T_K = \Theta/4$. The determinations of characteristic temperatures by resistivity and susceptibility data are in reasonably good agreement.

Pressure experiments indicate the importance of the pure volume effect. Jaccard *et al.*[8] investigated the resistivity of $CeCu_2Ge_2$ under pressure and found an increase of

$\rho(T^*)/\rho(T_{CF})$ as the applied pressure was increased up to 70 kbar, above which only one broad maximum was observed around 100 K. This resembles the resistivity behavior of CeCu$_2$(Si$_{1-x}$Ge$_x$)$_2$ as x increases. From the onset of superconductivity it has been concluded that CeCu$_2$Ge$_2$ under an external pressure of about 70 kbar behaves similar to CeCu$_2$Si$_2$ at ambient pressure. The 35 kbar curve[8] of CeCu$_2$Ge$_2$ has the largest $\rho(T^*)/\rho(T_{CF})$ ratio, in accordance with the CeCu$_2$(Si$_{0.5}$Ge$_{0.5}$)$_2$. The similarity holds even beyond $x=0$: The $\rho(T)$ curve of CeCu$_2$Ge$_2$ at around 100 kbar follows CeCu$_2$Si$_2$ near 30 kbar. Investigations[16] on CeCu$_2$Si$_2$ show that upon applying pressure the small maximum around 20 K moves to higher temperatures and finally merges with the feature at T_{CF} to a structureless anomaly resembling the behavior of typical high-T^* heavy-fermion systems.

In the range $T<T^*$ the resistivity decreases significantly before it levels off at around 1 K. For small x the resistivity drops smoothly down to 1 K, but for $x \geq 0.2$ slightly below the T^* maximum, we find a kink in $\rho(T)$ which monotonically moves to higher temperatures as x increases and can be identified as the Néel temperature T_N obtained by susceptibility experiments. Although less pronounced (in particular for $x \geq 0.4$), a second anomaly can be detected in $\rho(T)$ at around 2 K which seems to depend only weakly on x. This transition coincides with T_2 as detected in our susceptibility data. Slightly below 1 K, the slope of $\rho(T)$ changes again, indicating another transition labeled as T_3 in Fig. 6. The specimen of CeCu$_2$Si$_2$ becomes superconducting at 0.6 K (solid diamond in Fig. 6), confirming the high quality of our samples. At this point we are not certain about the continuation of the T_2 and T_3 as $x \to 0$. The continuation of T_N (long dashed line in Fig. 6) probably marks the boundary to the A phase[2] and does intersect at 0.75 K slightly above the superconducting transition.

At low temperatures a T^2 behavior of the resistivity $\rho(T)=\rho_0+AT^2$ is observed over a limited temperature range but well within the magnetically ordered phases. In the framework of Fermi-liquid theory, the prefactor A is proportional to γ^2 and $\chi^2(T \to 0)$, which was observed in a broad variety of materials.[32] For $x>0.1$, we found A to rapidly decrease by a factor of 10 up to $x \approx 0.6$; for larger x the prefactor A changes only slightly. These findings are in agreement with the results of specific heat measurements where $C_p/T(T=0)$ was reported to drop to one-third upon changing the Ge concentration from $x=0$ to $x=0.6$, while it is basically constant as the heavy-fermion behavior is gradually replaced by the regime of local magnetic moments on the Ge-rich side.[18] However, it is clear that for $x>0.1$, A can also be influenced by magnetic scattering processes. In CeCu$_2$Si$_2$ Bellarbi et al.[16] found that the range in which the T^2 law holds increases significantly with increasing pressure while the prefactor decreases.

From the high-temperature susceptibility measurements the effective magnetic moment μ_{eff} was evaluated by Eq. (1). The value $\mu_{eff}=(2.5 \pm 0.1)\mu_B$ is close to the free-ion Ce^{3+} value $2.54\mu_B$/Ce and indicates local magnetic moments of Ce^{3+}. It is in good agreement with the data reported on CeCu$_2$Si$_2$ (Ref. 33) and CeCu$_2$Ge$_2$,[14] but is in contrast to the value $\mu_{eff}=2.1\mu_B$ reported by deBoer et al.[34] In the low-

temperature range ($T<25$ K), the susceptibility also observes a Curie-Weiss behavior. The smaller value of μ_{eff} in this region can be explained by the crystal-field doublet ground state schemes proposed[28,35] for Ce^{3+}. The Curie temperature linearly decreases with concentration, while μ_{eff} increases with x.

The maximum of $\chi(T)$ defines the Néel temperature T_N, and magnetic ordering can clearly be observed for all concentrations $x \geq 0.2$. As displayed in Fig. 6, T_N monotonically increases as a function of x up to $T_N=4.1$ K in the case of CeCu$_2$Ge$_2$. This behavior is consistent with the depression of T_N as external pressure is applied upon CeCu$_2$Ge$_2$.[36] T_N slightly shifts to lower temperatures with increasing magnetic field as expected for an AFM ordering. As seen more clearly in the derivative of $\chi(T)$, an additional anomaly at $T_2 \approx 2$ K can be detected (Fig. 2) which we interpret as evidence of a subsequent phase transition. The transition temperatures for different x obtained by susceptibility experiments are indicated as triangles in the phase diagram of Fig. 6. For small x, T_N coincides with the maximum of $d\chi/dT$, but in the intermediate range of Ge concentration $0.4<x \leq 0.6$, the $d\chi/dT$ peak continues in the T_2 line while only a shoulder indicates T_N. On the Ge-rich side ($x \geq 0.9$) we do not find evidence for this transition which may indicate a critical point at $T=2.1$ K and $x=0.8$. This hypothesis is strongly supported by the results of our neutron scattering experiments which provide evidence that the same magnetic structure is present in CeCu$_2$Ge$_2$ between $T=1.5$ K and the Néel temperature $T_N=4.1$ K. At $T=1.6$ K, this magnetic order is also found for $x=0.8$ and 0.6 as indicated in Fig. 6 by the hatched area. The suggestion of Trovarelli et al.[18] that different magnetic structures show up in the intermediate regime is not supported by our experimental results, although it seems unlikely that the transition at T_2 is anything else but of magnetic origin. The data on the thermal expansion[12] have been interpreted[18] as showing some indications of transitions near 0.6 K and 2.3 K for $x=1$. These anomalies, however, are much less pronounced than the one at T_N. We feel that there is not sufficient evidence to extend the phase boundaries T_2 and T_3 beyond $x=0.8$.

The phase diagram as presented in Fig. 6 is yet unclear and can hardly be understood. At the Si-rich side, it seems that superconductivity is rapidly suppressed and followed by a phase in close analogy to the A phase in the B-T phase diagram.[6] Hence one may conclude that the regime embedded between the phase lines T_2 and T_3 is closely related to the A phase. However, this regime is also characterized ($x=0.6$ and 0.8) by the same magnetic order of the localized moments as in the pure CeCu$_2$Ge$_2$ compound which seems to be established along the phase boundary T_N. Clearly, T_2 is not characterized by a change of the spin alignment of the incommensurate phase which is established at T_N, but it is definitely a magnetic phase transition. We conclude that at the phase boundary T_2, a bandlike magnetism is established, in addition to the existing order of highly compensated but localized moments. We are aware of no theory to explain this coexistence of local-moment and band magnetism in heavy-fermion systems and we have to agree that this proposal is highly speculative. Finally, at the moment nothing can be said concerning the low-temperature phase $T<T_3$. Detailed

neutron experiments are currently undertaken to shed light on this fascinating phase diagram.

V. CONCLUSION

We have studied the magnetic phase diagram of the system $CeCu_2(Si_{1-x}Ge_x)_2$ with $0 \leq x \leq 1$ by electrical transport, magnetic susceptibility, and neutron scattering measurements. Three phase transitions are identified in the temperature range below 5 K. We found the Néel temperature T_N to increase continuously as x increases. In addition, in the range from $0.4 \leq x \leq 0.8$ a second anomaly was found at $T_2 \approx 2$ K. There are also indications of another low-temperature transition at around 0.5 K.

There are three regimes in the phase diagram which deserve further studies by complementary methods. In the vicinity of $x=0$ the coexistence or competition of the different phases has to be clarified. In the range $0.2 \leq x \leq 0.4$ the crossover, coexistence, or merging of the T_N and T_2 boundary is of interest. And finally, it is not clear whether the T_2 line halts near $x=0.8$ or continues towards $x=1$. Of equal importance is the question of the nature of both transitions T_2 and T_3. Additional temperature-dependent neutron diffraction and NMR studies are in progress to clarify some of the points mentioned.

ACKNOWLEDGMENTS

*Permanent address: BENSC Hahn-Meitner-Institut, D-14109 Berlin, Germany.

†Electronic address: di7o@hrzpub.th-darmstadt.de

[1] F. Steglich, J. Aarts, C. D. Bredl, W. Lieke, D. Meschede, W. Franz, and H. Schäfer, Phys. Rev. Lett. **43**, 1982 (1979).

[2] G. Bruls, B. Wolf, D. Finsterbusch, P. Thalmeier, I. Kouroudis, W. Sun, W. Assmus, B. Lüthi, M. Lang, K. Gloos, F. Steglich, and R. Modler, Phys. Rev. Lett. **72**, 1754 (1994).

[3] A. Amato, Physica B **199 & 200**, 91 (1994).

[4] R. Feyerherm, A. Amato, C. Geibel, F. N. Gygax, P. Hellmann, R. H. Heffner, D. E. MacLaughlin, R. Müller-Reisener, G. J. Nieuwenhuys, A. Schenck, and F. Steglich, Physica B **206 & 207**, 596 (1995).

[5] C. Geibel *et al.*, Z. Phys. B **83**, 305 (1993).

[6] F. Steglich, B. Buschinger, P. Gegenwart, C. Geibel, R. Helfrich, P. Hellmann, M. Lang, A. Link, R. Modler, D. Jaccard, and P. Link (unpublished).

[7] G. Knopp, A. Loidl, K. Knorr, L. Pawlak, M. Duczmal, R. Caspary, U. Gottwick, H. Spille, F. Steglich, and A. P. Murani, Z. Phys. B **77**, 95 (1989).

[8] D. Jaccard, K. Behnia, and J. Sierro, Phys. Lett. A **163**, 475 (1992).

[9] N. Büttgen, R. Böhmer, and A. Loidl, Solid State Commun. **93**, 753 (1995).

[10] Y. Kitaoka, H. Tou, G.-Q. Zheng, K. Ishida, K. Asayama, T. C. Kobayashi, A. Kohda, N. Takeshita, K. Amaya, Y. Onuki, C. Geibel, C. Schank, and F. Steglich, Physica B **206 & 207**, 55 (1991).

[11] N. Büttgen, R. Böhmer, A. Krimmel, and A. Loidl, Phys. Rev. B **53**, 5557 (1996).

[12] A. Loidl, A. Krimmel, K. Knorr, G. Sparn, M. Lang, C. Geibel, S. Horn, A. Grauel, F. Steglich, B. Welslau, N. Grewe, H. Nakotte, F. R. de Boer, and A. P. Murani, Ann. Phys. (Leipzig) **1**, 78 (1992).

[13] G. Sparn, P. C. Canfield, P. Hellmann, M. Keller, A. Link, R. A. Fisher, N. E. Phillips, J. D. Thompson, and F. Steglich, Physica B **206 & 207**, 212 (1995).

[14] G. Liang, R. Barber, Y. Tang, M. Croft, J. L. Cobb, and J. T. Markert, Phys. Rev. B **51**, 214 (1995).

[15] H. Spille, U. Rauchschwalbe, and F. Steglich, Helv. Phys. Acta **56**, 165 (1983).

[16] B. Bellarbi, A. Benoit, D. Jaccard, J. M. Mignot, and H. F. Braun, Phys. Rev. B **30**, 1182 (1984).

[17] F. Thomas, Physica B **186-188**, 303 (1993).

[18] O. Trovarelli, M. Weiden, R. Müller-Reisner, M. Gómez-Berisso, J. G. Sereni, C. Geibel, and F. Steglich (unpublished).

[19] W. Assmus, M. Herrmann, U. Rauchschwalbe, S. Riegel, W. Lieke, H. Spille, S. Horn, G. Weber, F. Steglich, and G. Cordier, Phys. Rev. Lett. **52**, 469 (1984).

[20] G. Liang and M. Croft, Phys. Rev. Lett **40**, 361 (1989).

[21] G. Liang, J. Chen, Y. Jeon, M. Croft, and A. S. Edelstein, Physica B **163**, 355 (1990).

[22] E. V. Sampathkumaran and R. Vijayaghavan, Phys. Rev. Lett. **56**, 2861 (1986).

[23] S. Foner, Rev. Sci. Instrum. **30**, 548 (1959).

[24] E. F. Bertaut, Acta Crystallogr. **23**, 73 (1968).

[25] O. Elsenhaus, J. Appl. Crystallogr. **23**, 73 (1990).

[26] J. A. Blanco, D. Gignoux, and D. Schmitt, Phys. Rev. B **43**, 13 145 (1991).

[27] J. A. Blanco, D. Schmitt, and J. C. Gómez Sal, J. Magn. Magn. Mater. **116**, 128 (1992).

[28] E. A. Goremychkin and R. Osborn, Phys. Rev. B **47**, 14 280 (1993).

[29] P. M. Levy and S. Zhang, Phys. Rev. Lett. **62**, 78 (1989).

[30] G. Grüner and A. Zawadowski, in *Progress in Low Temperature Physics*, edited by D. F. Brewer (North-Holland, Amsterdam, 1978), Vol. VII B, p. 591.

[31] G. Grüner and A. Zawadowski, Rep. Prog. Phys. **37**, 1497 (1974).

[32] A. Auerbach and K. Levin, Phys. Rev. B **34**, 3524 (1986).

[33] B. Batlogg, J. P. Remeika, and A. S. Cooper, J. Appl. Phys. **55**, 2001 (1984).

[34] F. R. deBoer, J. C. P. Klaasse, P. A. Veenhuizen, A. Böhm, C. D. Bredl, U. Gottwick, H. M. Mayer, L. Pawlak, U. Rauchschwalbe, H. Spille, and F. Steglich, J. Magn. Magn. Mater. **63 & 64**, 91 (1987).

[35] S. Horn, E. Molland-Moritz, M. Loewenhaupt, F. Steglich, H. Scheuer, A. Benoit, and J. Flouquet, Phys. Rev. B. **23**, 3171 (1981).

[36] G. Sparn, W. P. Beyermann, P. C. Canfield, Z. Fisk, J. D. Thompson, and F. Steglich, Int. J. Mod. Phys. B **7**, 54 (1993).